Real-time TIRF imaging of single adiponectin vesicle exocytosis in 3T3-L1 adipocytes stably expressing mCherry fused to human adiponectin

Man Mohan Shrestha[1], Sebastian Barg[2] and Charlotta S. Olofsson[1]

[1]Department of Physiology/Metabolic Physiology, Institute of Neuroscience and Physiology, Institute of Biochemistry, The Sahlgrenska Academy, University of Gothenburg, Göteborg, Sweden.

[2]Department of Medical Cell Biology, Uppsala University, Uppsala, Sweden.

Running title: *Imaging hormone exocytosis in live adipocytes*

To whom correspondence should be addressed: Dr Man Mohan Shrestha and Associate Professor Charlotta Olofsson, University of Gothenburg, The Sahlgrenska Academy, Dept. Neuroscience and Physiology, Section of Metabolic Physiology, Postal address: Box 432, SE-405 30 Göteborg, Sweden,

E-mail: Man Mohan Shrestha: man.shrestha@gu.se. Charlotta Olofsson: charlotta.olofsson@gu.se

Keywords: adiponectin, exocytosis, TIRF imaging, white adipocyte, chimeric protein expression

Abstract

Adiponectin is a peptide hormone abundantly released from adipocytes, and reduced circulating levels are associated with obesity-related diseases, such as type 2 diabetes, insulin resistance and cardiovascular disease. Adiponectin is released by regulated exocytosis of secretory vesicles, but traditional molecular biology and imaging techniques lack the specificity and time resolution to adequately quantify exocytosis and trafficking of adiponectin-containing vesicles. Here we generated 3T3-L1 adipocytes that stably express mCherry-tagged human adiponectin, resulting in robust labelling of small adiponectin vesicles with a diameter of 200-300 nm, in live cells. Total internal reflection fluorescence (TIRF) microscopy was used to visualise and quantify exocytosis and adiponectin release in real-time, observed as rapid disappearance of the fluorescence of individual vesicles. Bulk adiponectin secretion measurements confirmed that the labelled adiponectin was secreted to the surrounding solution under these conditions, and expressed in the same vesicle population as endogenous adiponectin. In contrast to previous electrophysiological results, elevation of cytosolic Ca^{2+} alone was sufficient to induce exocytosis, although at a lower rate compared to elevated cytosolic cAMP. We conclude that the adiponectin-mCherry-labelled cells are useful for studying adiponectin exocytosis at the single vesicle level, and that an intracellular elevation of either cAMP or Ca^{2+} can trigger adiponectin vesicle release.

Introduction

The adipocyte-derived hormone adiponectin has anti-diabetic, anti-atherogenic and anti-inflammatory effects and acts as an insulin sensitizer. Thus, adiponectin plays crucial roles in metabolic disorders, including insulin resistance, type 2 diabetes and cardiovascular disease (1, 2). Overexpression of adiponectin is associated with protection against both acute and chronic effects of high fat diet-induced lipotoxic effects of lipid accumulation, and enhances the metabolic flexibility of adipose tissue (3).

A number of studies support that adiponectin is secreted via regulated exocytosis of pre-formed adiponectin-containing vesicles. Lim et al. demonstrated the vesicular localisation of adiponectin and that insulin stimulates release of measurable amounts of adiponectin at time-points between 60 and 120 minutes (4). The insulin-induced secretion was unaffected by pre-incubation with the protein synthesis inhibitor cyclohexamide, indicating that the secretagogue stimulates release of vesicles belonging to a pool of already synthesised vesicle. Our own work has defined an alternate pathway for adiponectin exocytosis: By combining electrophysiological and biochemical techniques with mathematical modelling, we have demonstrated that adiponectin exocytosis is triggered by an increase of intracellular cAMP and activation of exchange factor directly activated by cAMP, isoform 1 (Epac1). The cAMP/Epac1-dependent adiponectin release occurs in the absolute absence of Ca^{2+} (shown by buffering with the Ca^{2+} chelator BAPTA), but is none the less potentiated by an elevation of cytosolic Ca^{2+}. This regulation of adiponectin exocytosis exists in cultured 3T3-L1 adipocytes as well as in primary mouse and human adipocytes. Membrane capacitance recordings (that measure exocytosis as the increase in plasma membrane area that occurs upon vesicle fusion) showed that the cAMP/Ca^{2+}-triggered adiponectin exocytosis can be detected within 1-2 min after intracellular addition of stimuli. The stimuli consisted of inclusion of cAMP with or without Ca^{2+} in the patch pipette solution washing into the recorded cell, or extracellular addition of the cAMP-elevating agent forskolin and/or the Ca^{2+} ionophore ionomycin (5-7). Later work demonstrated that pre-treatment of adipocytes with cyclohexamide was without effect also on the cAMP-triggered adiponectin secretion (8). Collectively, our work proposes that pre-stored adiponectin vesicles undergo rapid exocytosis upon stimulation with cAMP in both the presence and absence of Ca^{2+}, in agreement with the cell model in Fig. 1.

Total internal reflection fluorescence (TIRF) microscopy is an optical technique that enables the excitation of fluorophores in a very narrow optical section. TIRF microscopy provides a means to selectively excite fluorophores near the adherent cell surface, while counter-

74 minimizing fluorescent signals from other intracellular regions (10). The narrow TIRF
75 excitation field allows high-resolution visualisation of processes occurring near or in the
76 plasma membrane, in live cells (11). Thus, by applying TIRF microscopy to adipocytes
77 expressing a fluorophore localised to adiponectin vesicles, their exocytosis can be visually
78 observed at single cell and single vesicle level, at high spatial and temporal resolution.

79 Here, we describe the generation of 3T3-L1 cells that stably express mCherry fused to the C-
80 terminal end of human adiponectin, to produce a genetically homogenous clonal cell population
81 that over-express the recombinant protein of interest. We demonstrate that the adiponectin-
82 mCherry expressing cells can be differentiated into mature adipocytes, as judged by lipid-
83 filling. Using TIRF microscopy, we can visualise and quantify Ca^{2+} and cAMP-triggered
84 adiponectin exocytosis in real-time, at the single-vesicle resolution.

85 Material and methods

86 Safety and Handling of Recombinant Lentiviruses

87 All the lentiviruses were generated using a third generation packaging system as per Biosafety
88 Level 2 and institutional guidelines of the University of Gothenburg. Disposable plastic
89 pipettes were used and liquid waste was decontaminated with 10 % bleach. Laboratory
90 materials in contact with viral particles were treated as biohazardous waste and autoclaved.

91 Cell culture

92 HEK293T (ATCC) cells were cultured in high glucose DMEM (Invitrogen, GIBCO)
93 supplemented with 10 % fetal bovine serum (FBS) and 1 % penicillin-streptomycin at 37 ^{0}C
94 and 5 % CO_2. Cultured clonal 3T3-L1 fibroblasts (Zenbio) were seeded and differentiated into
95 mature adipocytes and used for experiments at day 8 or 9 according to previous establish
96 protocol (7). In brief, 3T3-L1 fibroblasts were cultured in high glucose DMEM (Invitrogen,
97 GIBCO) supplemented with 10 % new born calf serum at 37 ^{0}C and 5 % CO_2. Two days after
98 confluence, cells were washed twice with warm PBS and a differentiation medium containing
99 10 % FBS, 1 % penicillin-streptomycin, 0.85 μM insulin, 0.5 mM 3-isobutyl-1-methylxanhine
100 and 1 μM dexamethasone was added for 2 days. The differentiation medium was there after
101 replaced with medium containing 10 % FBS and insulin for another 2 days. Cells were then
102 maintained in DMEM with 10 % FBS. Adipocytes were used for experiments on day 8 or 9

103 post differentiation. Only 3T3-L1 adipocytes that appeared mature, as judged visually by
104 accumulated lipid, were studied.

105 **Generation of lentiviral constructs**

106 Three candidate hairpin sequences for mouse adiponectin (NM_009605.5) each containing 21
107 sense bases that are identical to the target gene, a loop containing an XhoI restriction site and
108 21 antisense bases that are complementary to the sense bases followed by a poly T termination
109 sequence, were designed using an small interfering RNA (siRNA) selection tool hosted by the
110 Whitehead Institute for Biomedical Research (http://sirna.wi.mit.edu/) (12). Starting at 25nt
111 downstream of the start codon (ATG), we searched for 21nt sequences that matched the pattern
112 AA(N19). It was ascertained that the G-C content was >35 %. To minimize degradation of off-
113 target mRNAs, the NCBI's BLAST program was used. Since some sequences are likely more
114 effective than others, multiple target sequences were selected for the *Acrp30* gene (Table 1).

115 The annealed oligos were inserted into an empty backbone third generation transfer plasmid
116 (pLKO.1-TRC cloning vector; Plasmid #10878; addgene) using AgeI (5' cloning site) and
117 EcoRI (3' cloning site) restriction digestion sites. Similarly, a candidate hairpin sequence for
118 green fluorescent protein (GFP) was used for a control/scramble (pLKO.1 GFP; Plasmid
119 #30323; addgene). mCherry fused to human adiponectin (hAcrp30-mCherry) was cloned into
120 a pLenti vector using NheI and HpaI restriction digestion sites to generate lentiviral constructs
121 (Supplementary Fig. 1A). The sequences of the knockdown and lentiviral constructs were
122 verified using restriction digestion and Sanger's Sequencing from Eurofins Genomics.

123 **Lentivirus Packaging and Infection**

124 Lentiviruses were produced by co-transfection of HEK293T cells with lentiviral expression
125 and packaging plasmids using the calcium phosphate transfection method (13, 14). Viral
126 supernatant was collected after 48 hours of transfection, centrifuged at 1,000 x g for 5 minutes
127 and filtered through 0.45 µm filter. The viruses were further concentrated by ultracentrifugation
128 using Ti45 rotor in Beckman Coulter Optima-L-100 XP at 116,000 x g for 2 hours at 4 °C. For
129 gene silencing, 3T3-L1 fibroblasts were transduced with titrated viruses in presence of 8 µg/mL
130 of polybrene (Hexadimethrine bromide, Cat. No: 107689-10G, Sigma-ALDRICH) and
131 subjected to antibiotic selection using 4 µg/mL puromycin after 48 hours. The successful stable
132 expression was verified by fluorescence microscopy for fusion proteins whereas knockdown
133 efficiency was assessed by Western blotting and RT-qPCR at protein and mRNA level

134 respectively. For generation of a stably expressing mCherry fused adiponectin cell line, 3T3-
135 L1 fibroblasts were infected with optimum amount of viral particles in the presence of
136 polybrene. The growth medium was changed 24 hours after infection.

137 **Adiponectin secretion**

138 3T3-L1 cells stably expressing adiponectin-mCherry were seeded and differentiated into
139 mature adipocytes on 35 mm glass bottom dish (D35-20-1.5-N, Cellvis). The mature
140 adipocytes were incubated with an extracellular solution containing 140 mM NaCL, 3.6 mM
141 KCL, 0.5 mM $MgSO_4$, 0.5 mM NaH_2PO_4, 2.0 mM $NaHCO_3$ and 5.0 mM Hepes (pH 7.4)
142 supplemented with 2.6 mM $CaCl_2$ and 5.0 mM glucose for 30 minutes at 32 °C. Test substances
143 were added for 30 min at 32 °C under gentle shaking. At termination of the incubation, the
144 medium containing secreted product was collected, and the adipocytes were lysed using PBS
145 containing 2 % SDS and protease inhibitor (1 tablet per 10 mL; cOmplete Mini, Roche
146 Diagnotics). Secretion samples were centrifuged for 5 minutes at 2000 rpm and 4 ^{0}C, and the
147 supernatant was stored at -80 °C. Secreted HMW and total adiponectin (measured with HMW
148 and Total Adiponectin ELISA (human) kit, 47-ADPMS-E01, Alpco) were expressed in relation
149 to total protein content. Cell lysates were centrifuged at 14000 rpm for 10 minutes at 4 ^{0}C and
150 total protein contents were measured by Bradford protein assay.

151 **Lipolysis Assays**

152 Matured adipocytes were incubated with an extracellular (EC) solution for 30 minutes at 32
153 °C. Lipolysis was stimulated by adding the adenylate cyclase activator Forskolin (10 µM) and
154 the phosphodiesterase inhibitor isobutylmethylxanthine (IBMX) (200 µM) or Ionomycin
155 (1 µM) in serum-free extracellular (EC) solution for 30 min at 32 °C under gentle shaking. At
156 termination of the incubation, the medium containing secreted product was collected, and the
157 adipocytes were lysed using PBS containing 2% SDS and protease inhibitor (1 tablet per 10
158 mL; cOmplete Mini, Roche Diagnotics). Cell lysates were centrifuged at 14000 rpm for 10
159 minutes at 4 ^{0}C and total protein contents were measured by Bradford protein assay. Secretion
160 samples were centrifuged for 5 minutes at 2000 rpm and 4 ^{0}C, and the supernatant was
161 collected. Lipolysis was assessed from the release of FFA and glycerol in the secretion samples
162 using non-esterified fatty acids measurement kit (FUJIFILM Wako Chemicals Europe GmbH)
163 and free glycerol reagents (G7793 and F6428, Sigma) respectively and normalised to total
164 protein contents.

165 **Real-Time Quantitative PCR**

166 RNA was extracted and purified using QIAzol (Qiagen) and ReliaPrep RNA Cell MiniPrep
167 System (Promega). 1 µg of RNA was used for reverse transcription. cDNA synthesis was
168 performed according to the protocol as described in Invitrogen^{TM} SuperScript^{TM} II Reverse
169 Transcriptase kit (Thermo Fisher Scientific #18064022) in presence of 40 units of
170 RNaseOUT^{TM} Recombinant Ribonuclease Inhibitor (Thermo Fisher Scientific #10777-019)
171 and 200 units of Reverse Transcriptase per 20 µL of reaction mixture. The real-time
172 quantitative PCR (qPCR) assays were performed using Fast SYBR Master Mix (4385612,
173 Applied Biosystems). The relative expression of mRNA abundance was calculated using $2^{-\Delta\Delta Ct}$
174 and was normalized to β-actin. Data are represented as mean ± SEM, ****$p<0.0001$ (n=3).

175 **Western blotting**

176 3T3-L1 adipocytes were lysed with TNET buffer (50 mM Tris-HCl, pH 7.5, 150 mM NaCl, 10
177 mM NaF, 1 mM EDTA and 1% Triton X-100) containing 2 mM Na_3VO_4 (Sodium
178 Orthovanadate) and 1 mM pmsf (phenylmethylsulfonyl fluoride) and 1x protease inhibitor
179 cocktail tablet (Roche). Whole cell lysates were centrifuged at 12,000 rpm at 4 ^{0}C for 10
180 minutes. The protein concentration was determined using Bradford protein assay. Proteins
181 from whole cell lysate (20 µg) were separated by 8 % sodium dodecyl sulfate polyacrylamide
182 gel electrophoresis (SDS/PAGE) and then transferred onto polyvinylidene difluoride (PVDF)
183 membranes (Millipore) at 120 V for 2 hours using transfer buffer (25 mM Tris-base, pH 8.3,
184 190 mM glycine, 20 % methanol and 0.1 % SDS). After blocking in blocking buffer (2 % BSA
185 in PBS containing 0.2 % Tween-20 and 0.01 % sodium azide) for 1 hour at room temperature,
186 the membrane was incubated overnight at 4 ^{0}C with primary antibody against adiponectin
187 (ab3455, Abcam) and tubulin (T9026, Sigma) as loading control at 1:1000 dilution. The
188 primary antibodies were probed using HRP-conjugated secondary antibodies at 1:5000 dilution
189 and detection was performed with enhanced chemiluminescence.

190 **Live Cell imaging using TIRF microscopy and analysis of vesicle exocytosis**

191 3T3-L1 adipocytes expressing hAcrp30-mCherry were pre-treated with extracellular solution
192 for 30 minutes at 32 °C and kept in the same solution supplemented with 2.6 mM $CaCl_2$ and
193 5.0 mM glucose during imaging. Image acquisition was performed by TIRF Observer Z1
194 microscope with alpha Plan-Apochromat 100×/1.46 Oil objective (both Carl Zeiss) and an
195 EMCCD camera (Evolve 512 delta, Photometrics). Images were acquired using Zeiss Zen 2.6

196 (blue edition). Excitation laser of wavelength 561 nm with exposure time 25–100 ms was used
197 for mCherry. Forskolin together with the phosphodiesterase inhibitor 3-isobutyl-1-
198 methylxanthine (FSK/IBMX) or ionomycin alone were added 1–2.5 minutes after acquisition
199 start and the time point was noted. TIRF images were acquired over 15 minutes at 2 Hz through
200 1801 total readings. Circles of region of interest (ROI) around the vesicles were used to
201 measure the fluorescence intensities of images over time. All the readings were normalized to
202 the intensity measured at time point zero, after removal of the background fluorescence. Values
203 were plotted against time, so as to indicate the time course of adiponectin containing vesicle
204 exocytosis. Vesicle size was estimated using fluorescent polystyrene beads of known diameter.
205 Vesicle locations were found by eye, a 21 pxl long line was centered on this location, and the
206 brightness along this line was read out ("linescan"). The following piecewise linear function
207 describing a trapezoid shape was then fitted to the linescan to estimate spot width: if ($x1<$
208 $x<x1+bl$) $y=a+s*(x-x1)$; if ($x2-bl< x<x2$) $y=a+s*(x2-x)$; if ($x1+bl<x<(x2-bl)$ $y=a+s*bl$; else
209 $y=a$, where x1 and x2 are boundaries of the peak, a the peak amplitude, s the slope, bl the width
210 of the two sloped sections, and y the brightness. The apparent width is $w=x2-x1-bl$, which is
211 the full width at half maximum (FWHM) of the trapezoid. bl was fixed to 1.5pxl (240nm), the
212 theoretical resolution of the system. Beads with known diameters were imaged and measured
213 in the same way, to create a reference scale.

214 **Analysis**

215 Images were analysed using Zeiss Zen 2.6 (blue edition) and OriginPro (OriginLab
216 Corporation). All data are presented as mean values ± SEM for designated number of
217 experiments. Significance of difference was tested by Student's t-test and ANOVA. Statistical
218 analysis were performed using Prism 9.0 (GraphPad, San Diego, CA).

219

220 # Results

221

222 **Knock down and rescue of endogenous adiponectin in 3T3-L1 adipocytes**

223 3T3-L1 cells with low passage number were used and it was ascertained that the cells were
224 able to express high levels of endogenous adiponectin when differentiated into adipocytes
225 (Fig. 2A). To avoid that native adiponectin interferes with the expression of human
226 adiponectin-mCherry, the endogenous adiponectin was knocked down by short hairpin RNA
227 (shRNA). Three different target sequences for shRNA mouse adiponectin knockdown were

228 designed: shAcrp30-A, shAcrp30-B and shAcrp30-C (Table 1). The targets were inserted into
229 a lentiviral plasmid and 3T3-L1 fibroblasts were transduced with the viral particles. The
230 transduced cells were thereafter differentiated into mature adipocytes. For two out of three
231 knockdowns (shAcrp30-A and shAcrp30-C) transduced cells could be cultured into mature
232 adipocytes, whereas cells transduced with shAcrp30-B did not survive. The successful
233 knockdown was confirmed by protein and gene expression, where adiponectin gene
234 knockdown was compared with scrambled shRNA targeting GFP (Fig. 2B-D).
235
236 Cells that displayed the most efficient knockdown (shAcrp30-A), were rescued with hAcrp30-
237 mCherry alone (plasmid map in Suppl. Fig. 1) or with a FLAG tag either at the N- or C-terminal
238 in the fibroblast stage. (The FLAG was added to allow future protein purification by affinity
239 chromatography as well as localisation of the fusion protein in live cells.) The rescued cells
240 were seeded and differentiated into mature adipocytes, and the over-expression of hAcrp30
241 was verified by Western blotting using antibodies against adiponectin or FLAG. The hAcrp30-
242 mCherry tagged with FLAG at the C-terminal was found to be highly over-expressed compared
243 to the other two variants under both reduced (Fig. 3A) and non-reduced (Fig. 3B) conditions.
244 The over-expression of adiponectin-mCherry was visualized by inverted fluorescence
245 microscope (Fig. 3C) and TIRF microscopy (Fig. 3D); TIRF imaging demonstrated a punctate
246 pattern of fluorescence, as typical for vesicular compartments. Most of the labelled vesicles
247 appeared diffraction limited or slightly larger in size. Comparing the apparent width (FWHM)
248 of the vesicles with that of fluorescently labelled beads of known diameter allowed us to
249 estimate their median diameter to ~200-300 nm (Fig. 3E, F).
250
251 **An elevation of intracellular cAMP or Ca^{2+} triggers exocytosis of mCherry-labelled**
252 **adiponectin vesicles**
253 We have shown that a combination of the adenylyl cyclase activator forskolin and the
254 phosphodiesterase inhibitor 3-isobutyl-1-methylxanthine (FSK/IBMX) increases 3T3-L1
255 adipocyte cAMP levels >6-fold (7), and that the Ca^{2+} ionophore ionomycin elevates the
256 intracellular Ca^{2+} level ($[Ca^{2+}]_i$; (6). Thus, we investigated adiponectin vesicle exocytosis in
257 differentiated 3T3-L1 adipocytes stably expressing adiponectin-mCherry exposed to
258 FSK/IBMX or ionomycin. As shown in Fig. 4A, addition of FSK/IBMX led to disappearance
259 of mCherry-labelled vesicles (bottom images in Fig. 4A and Suppl. video 1). A rapid loss of
260 fluorescence puncta was observed upon stimulation, which we interpreted as exocytosis events
261 (top row Fig. 4C and Fig. 4D). Approx. 60% of the vesicles observed by TIRF microscopy

262 fused with the plasma membrane after addition of the stimulatory agents, while the remaining
263 40% were stable throughout the recording (middle row Fig. 4C and Fig. 4E). This is expected
264 since it is unlikely that all adiponectin vesicles that reside close to the plasma membrane, within
265 the TIRF zone, are primed for exocytosis (15). In experiments with adipocytes exposed to the
266 control solution during the entire experiment (Fig. 4B and Suppl. video 2), the labelled
267 adiponectin vesicles remained stable throughout the TIRF recording (bottom row Fig. 4C).
268 Calculation of the fraction of released vesicles confirmed that a larger number of vesicles were
269 exocytosed upon exposure to the cAMP-elevating agents compared to control (Fig. 4F). At the
270 end of 15 min recordings, significantly fewer adiponectin-mCherry labelled vesicles remained
271 in adipocytes exposed to FSK/IBMX, compared to control solution (Fig. 4G).
272
273 Ionomycin likewise triggered the exocytosis of adiponectin-containing vesicles (Fig. 5A, and
274 Suppl. video 3). Similar to the experiments with FSK/IBMX, a rapid loss of fluorescence
275 puncta was observed upon stimulation, indicating vesicle exocytosis (top row Fig. 5C and
276 Fig. 5D) and a fraction of adiponectin-containing vesicles remained stable throughout the
277 recording (middle row Fig. 5C and Fig. 5E). It was again confirmed that adiponectin-mCherry
278 vesicles remained stable in adipocytes maintained in control solution (Fig. 5B, bottom row
279 Fig. 5C and Suppl. video 4). The fraction of released vesicles was significantly larger in the
280 ionomycin-exposed adipocytes compared to control experiments, at all investigated time-
281 points (Fig. 5F). Significantly fewer adiponectin-mCherry labelled vesicles remained in
282 ionomycin-exposed adipocytes compared to control cells, at the end of 15 minute recordings
283 (Fig. 5G). As can be seen upon comparison of Figs. 4F and 5F, whereas 60% of the vesicles
284 residing in the TIRF zone were released after 10 min exposure to FSK/IBMX, the
285 corresponding fraction of secreted vesicles amounted to only 15% in ionomycin-treated
286 adipocytes.
287
288 **Measurements of released adiponectin, FFA and glycerol in 3T3-L1 adipocytes stably**
289 **expressing adiponectin-mCherry**
290 To verify the adiponectin secretion capacity of the stably expressing 3T3-L1 cells, the matured
291 adipocytes were incubated in the presence of FSK/IBMX or ionomycin and product secreted
292 to the medium was measured by ELISA. In agreement with previous results (6, 7) the
293 secretagogues stimulated the release of mouse adiponectin in native 3T3-L1 adipocytes
294 (Fig. 6A). The 3T3-L1 adipocytes stably expressing adiponectin-mCherry likewise secreted
295 adiponectin in response to both FSK/IBMX and ionomycin and both total (Fig. 6B) and the

296 high-molecular weight (HMW) form (Fig. 6C) of human adiponectin were released over basal
297 (unstimulated control cells). The data confirm that the stably expressing adipocytes secrete
298 smaller and larger forms of the adiponectin-mCherry fusion protein in response to cAMP or
299 Ca^{2+} stimulation, at levels similar to that observed in mouse native adipocytes. To further
300 validate the functionality of in the adiponectin-mCherry adipocytes, we measured release of
301 free fatty acids (FFA) and glycerol. FSK/IBMX elevated levels of both FFA and glycerol in
302 the incubation medium whereas ionomycin was without effect of release of either of the lipid
303 metabolites (Figs. 6D, E).
304

305 ## Discussion

306

307 Pre-stored neurotransmitter- or hormone-containing vesicles typically release their content to
308 the extracellular space upon receiving the correct triggering signal. Classically, an elevation of
309 cytosolic Ca^{2+}, released from intracellular stores or entering via Ca^{2+}-permeable ion channels
310 in the plasma membrane, stimulates vesicle exocytosis. Other intracellular mediators such as
311 cAMP and ATP also have important roles for vesicle maturation steps (15). Peptide hormone
312 exocytosis has been detailed in a number of endocrine cell types, including insulin secreting
313 beta-cells (16) and catecholamine-releasing chromaffin cells (17). However, the control of
314 hormone release in white adipocytes is a research field that has received little attention.
315 Adiponectin, one of the chief hormones secreted from white adipocytes and the most abundant
316 protein present in serum (18), has in several studies been reported to have favourable metabolic
317 effects and to protect from development of obesity-associated metabolic diseases (1, 2).
318 Although the general control of adiponectin secretion over shorter and longer time-periods has
319 been addressed in a small number of studies (4, 19-21), adiponectin vesicle exocytosis – the
320 molecular and cellular process in which adiponectin-containing vesicles are recruited to and
321 fuse with the adipocyte plasma membrane to release their cargo - is a largely unexplored field.
322 Here we have generated 3T3-L1 cells stably expressing human adiponectin fused with the
323 fluorescent protein mCherry, and we use the overexpressing matured adipocytes to visualise
324 and quantify adiponectin exocytosis. We demonstrate that adiponectin vesicle trafficking and
325 exocytosis can be studied at the single vesicle level, and we determine that an elevation of
326 intracellular Ca^{2+} stimulates adiponectin vesicles exocytosis in the absence of a concomitant
327 increase of cAMP. Below we discuss the usefulness of our cells for future studies of

328 adiponectin vesicle behaviour, and we reconsider the Ca^{2+}-dependence of adiponectin
329 exocytosis.
330
331 **The adiponectin-mCherry protein is targeted to endogenous adiponectin vesicles that**
332 **resemble hormone-containing vesicles in other endocrine cell types**
333 The addition of a fluorescent tag to a protein may disturb the correct targeting of the product.
334 Our TIRF data propose that the chimeric protein is present in vesicular compartments, indicated
335 by the punctate appearance of the fluorescence signal. Moreover, the real-time recordings
336 suggest that the overexpressing adipocytes are functional, and that adiponectin-mCherry is
337 targeted to the correct vesicle population; this is shown by that the labelled vesicles fuse with
338 the plasma membrane in response to signals known to stimulate adiponectin exocytosis. In
339 further support of this, measurements of released human adiponectin show that the fusion
340 protein is secreted in response to an elevation of cAMP or Ca^{2+}. Our estimated diameter of
341 200-300 nm for the adiponectin-labelled vesicles is similar to hormone-containing vesicles in
342 other endocrine cell types, such as insulin granules with a diameter of ~300 nm (26).
343
344 We have previously demonstrated that secretion of the hormones leptin, apelin and adipsin is
345 unaffected by cAMP in 3T3-L1 adipocytes (5) and that resistin is co-secreted with adiponectin
346 (contained within the same vesicles (37)). Collectively, our data propose that the rapid loss of
347 fluorescence puncta in response to cAMP or Ca^{2+} reflects exocytosis of single vesicles
348 belonging to the endogenous adiponectin vesicle population.
349
350 **Both cAMP and Ca^{2+} trigger exocytosis of adiponectin-mCherry labelled vesicles**
351 The real-time imaging data in Figs. 4 and 5, as well as Suppl. videos 1 and 3, confirm the
352 previously shown importance of cAMP and Ca^{2+} for stimulation of adiponectin vesicle release
353 (5-7, 27). However, the results in Fig. 5 and Suppl. video 3, where ionomycin triggers
354 exocytosis in the absence of a cAMP increase, can appear to contradict previous experiments
355 showing that Ca^{2+} alone is unable to induce exocytosis in 3T3-L1 adipocytes (6, 7). Notably,
356 there are some important difference between our previous patch-clamp data and the current
357 TIRF recordings: During the electrophysiological experiments, the interior of the adipocyte is
358 controlled by the pipette solution – thus by exclusion of cAMP in the pipette solution washing
359 into the cell, the experimental approach applied in (6, 7), the 3T3-L1 adipocytes can essentially
360 be depleted of cAMP. In contrast, the adipocytes used for TIRF imaging are metabolically
361 intact and have a continuous endogenous production of cAMP, maintaining basal levels of the

362 cyclic nucleotide. We suggest that the elevated Ca^{2+} acts together with preserved endogenous
363 levels of cAMP, to stimulate adiponectin exocytosis in micro-domains where cAMP is
364 sufficiently high. The finding that ionomycin on its own stimulates adiponectin secretion in
365 metabolically intact adipocytes is in agreement with data on secretion of the adipocyte hormone
366 resistin (28); we recently showed that resistin is co-secreted with adiponectin in mouse
367 adipocytes (thus contained within the same vesicles) and that ionomycin induced the release of
368 resistin in the absence of a cAMP-elevating agent (29). An alternative explanation to the effect
369 of ionomycin alone is that the increase in intracellular Ca^{2+} activates Ca^{2+}-dependent adenylyl
370 cyclases leading to production of cAMP. In Musovic et al. 2021, we were unable to demonstrate
371 a significant increase of cAMP levels in 3T3-L1 adipocytes exposed to ionomycin (Fig. 1C of
372 (29)). However, cAMP was measured in cell lysates, with no information of changes of cAMP
373 confined to specific near-membrane regions. Thus, ionomycin might stimulate local elevations
374 of cAMP, at sites of adiponectin vesicle exocytosis. It is well known that cAMP is
375 compartmentalised in adipocytes and that this regulates several intracellular processes (30). A
376 role of caveolae for the spatial control of cAMP has been demonstrated in cardiac myocytes,
377 and proposed to be relevant for βAR signalling (31). We have previously shown that caveolae
378 are necessary for the organisation of signalling pathways involved in the regulation of HMW
379 adiponectin exocytosis (32).
380
381 Vesicles that contain peptide/protein hormones typically undergo a series of maturation steps
382 including physical movement, docking (stable attachment to the plasma membrane) and
383 priming (chemical modifications that make docked vesicles release competent) before they can
384 discharge their cargo upon fusion with the plasma membrane (15). The data in Figs. 4 and 5 as
385 well as supplementary videos 1 and 3, show that both cAMP and Ca^{2+} trigger exocytosis of
386 adiponectin vesicles that are already docked at the adipocyte plasma membrane; no new
387 vesicles (newcomers) are observed to enter the TIRF zone. This observation seems to stand in
388 conflict with our previous electrophysiological data demonstrating that an elevation of Ca^{2+}
389 maintains adiponectin secretion over time, and with our conclusion that Ca^{2+} induces vesicle
390 replenishment. In this context, it is essential to keep in mind that we image only a small part
391 of/near the adipocyte plasma membrane, the ventral side of the cell attached to the culture dish,
392 whereas the capacitance recording reflect exocytosis that occur over the entire cell membrane.
393 Consequently, vesicles that move to and undergo exocytosis at the apical side of the adipocyte,
394 outside of the TIRF imaging zone, are not visualised.

395

396 **Choice of cells and fluorescent protein**

397 3T3-L1 cells were used to generate the adiponectin-mCherry expressing adipocytes. A number
398 of studies have demonstrated that *in vitro* differentiated 3T3-L1 adipocytes are a relevant cell
399 model for investigations of the adiponectin secretion process (5-7, 9, 22). In fact, all
400 mechanisms and mediators determined to regulate adiponectin exocytosis in 3T3-L1
401 adipocytes have been confirmed in primary mouse and human adipocytes ((7-9) and Musovic
402 & Olofsson, unpublished data). The 3T3-L1 cells are easy to culture and differentiate, and their
403 functionality with regard to adipocyte metabolic processes, such as lipolysis (23) and glucose
404 uptake (24), is well determined. Nonetheless, they are clonal cells and we acknowledge that
405 results must be continuously validated in experiments with primary, preferably human,
406 adipocytes. A disadvantage with the 3T3-L1 adipocytes is that their ability to differentiate into
407 mature adipocytes ceases with increased cell passage. Although multiple vials of low passage
408 cells can be stored, it will eventually be necessary to produce new stably expressing 3T3-L1
409 cells. However, we are not aware of any adipocyte cell line that does not have this limitation.
410 Collectively, we regard the 3T3-L1 adipocytes to be a good choice for our studies.

411

412 A large number of fluorescent proteins are available for protein tagging and real-time studies
413 of their specific function. The continuous development of fluorescent proteins with enhanced
414 or altered qualities have yielded a supply that covers the full visible spectrum, with diverse
415 advantages and disadvantages. Introduced nearly a decade ago, mCherry remains a frequently
416 used fluorescent marker for cellular studies. The mCherry has several advantages: It is bright
417 and it matures rapidly, enabling experiments to be performed soon after initiation of expression.
418 It is also highly photostable and resistant to photobleaching (25). Since experiments must be
419 carried out at high time-resolution and over an extended time-period (up to 30 min) the listed
420 qualities are important. We therefore labelled adiponectin with mCherry, expressed under the
421 CMV promoter that has high housekeeping expression. Human adiponectin was chosen to
422 enable us to biochemically distinguish between endogenous mouse adiponectin and the
423 overexpressed fusion protein. Nonetheless, there are some disadvantages related to using
424 mCherry for studies of adiponectin exocytosis: Red fluorescent proteins display limited pH
425 sensitivity compared to e.g. enhanced green fluorescent protein (EGFP) or pHluorin. Upon
426 vesicle fusion with the plasma membrane the pH of the vesicle lumen (which is acidic)
427 increases; pH-sensitive fluorescent proteins will consequently increase in brightness already
428 upon formation of the vesicle-plasma membrane fusion pore, thus confirming vesicle fusion.

429 For this reason, we initially evaluated the use of EGFP for studies of adiponectin exocytosis,
430 but both the more rapid photobleaching of EGFP, and lipid autofluorescence interfering with
431 the green signal complicated the studies. With regard to pHluorin, this optical indicator is non-
432 fluorescent at low pH and thus does now allow investigations of events that occur prior to
433 vesicle fusion with the plasma membrane. We nonetheless acknowledge the advantage of using
434 a pH-sensitive fluorescent tag for studies of vesicle fusion and cargo release and we will
435 evaluate their use for future investigations of the adiponectin exocytosis process. We also
436 recognise that tagging adiponectin itself might interfere with both protein mulitmerisation and
437 the secretion process. However, the secretion data confirm that the stably expressing adipocytes
438 release abundant amounts of human HMW adiponectin, verifying multimerisation of the
439 chimeric protein. Regardless of this, it would be valuable to assess if labelling of another
440 exocytosis vesicle marker such as Neuropeptide Y (NPY), a proven reliable marker for insulin
441 granule exocytosis (25), is useful for real-time imaging of the adiponectin vesicle release
442 process.
443
444 **What can we learn about the control of adiponectin secretion by real-time TIRF imaging**
445 **of adiponectin exocytosis?**
446 Our previous work has begun to detail the white adipocyte adiponectin exocytosis process (5-
447 9, 22, 27, 33). However, the combination of methods used have temporal and spatial limitations
448 and detailed knowledge of adiponectin vesicle dynamics and release can only be gained by
449 high-resolution imaging in live cells. The finding that adiponectin exocytosis is similarly
450 controlled in 3T3-L1 and primary mouse and human adipocytes (5, 7-9, 32, 33) open
451 opportunities to use the stably expressing cells to achieve a comprehensive understanding of
452 mechanisms and mediators that control adiponectin vesicle exocytosis, at the cellular and
453 molecular level. TIRF movies can be acquired at high time resolution (10-20 FPS), thus
454 allowing real time direct visualisation of the adiponectin vesicle exocytosis process.
455 Consequently, the control and rate of docking and exocytosis can be determined.
456
457 In summary, TIRF imaging of cultured or primary live adipocytes with fluorescently labelled
458 adiponectin vesicles will enable us, and others, to define currently unknown regulatory steps
459 of adiponectin vesicle dynamic, maturation and exocytosis, at a level of detail that has not been
460 studied previously. How are adiponectin vesicles recruited to the exocytosis site? Are the
461 vesicles present before, during and after exocytosis? Do vesicles interact with each other during

462 the exocytosis process? Those are questions that can be answered with the type of research
463 presented here.
464

465 **References**

466 1. Straub LG, Scherer PE. Metabolic Messengers: Adiponectin. Nat Metab. 2019;1(3):334-
467 9.
468 2. Iwabu M, Okada-Iwabu M, Yamauchi T, Kadowaki T. Adiponectin/AdipoR Research and
469 Its Implications for Lifestyle-Related Diseases. Front Cardiovasc Med. 2019;6:116.
470 3. Combs TP, Pajvani UB, Berg AH, Lin Y, Jelicks LA, Laplante M, et al. A transgenic mouse
471 with a deletion in the collagenous domain of adiponectin displays elevated circulating adiponectin and
472 improved insulin sensitivity. Endocrinology. 2004;145(1):367-83.
473 4. Lim CY, Hong W, Han W. Adiponectin is released via a unique regulated exocytosis
474 pathway from a pre-formed vesicle pool on insulin stimulation. Biochem J. 2015;471(3):381-9.
475 5. Brannmark C, Lovfors W, Komai AM, Axelsson T, El Hachmane MF, Musovic S, et al.
476 Mathematical modeling of white adipocyte exocytosis predicts adiponectin secretion and quantifies
477 the rates of vesicle exo- and endocytosis. J Biol Chem. 2017;292(49):20032-43.
478 6. El Hachmane MF, Komai AM, Olofsson CS. Cooling Reduces cAMP-Stimulated
479 Exocytosis and Adiponectin Secretion at a Ca2+-Dependent Step in 3T3-L1 Adipocytes. PLoS One.
480 2015;10(3):e0119530.
481 7. Komai AM, Brannmark C, Musovic S, Olofsson CS. PKA-independent cAMP stimulation
482 of white adipocyte exocytosis and adipokine secretion: modulations by Ca2+ and ATP. J Physiol.
483 2014;592(Pt 23):5169-86.
484 8. Komai AM, Musovic S, Peris E, Alrifaiy A, El Hachmane MF, Johansson M, et al. White
485 Adipocyte Adiponectin Exocytosis Is Stimulated via beta3-Adrenergic Signaling and Activation of
486 Epac1: Catecholamine Resistance in Obesity and Type 2 Diabetes. Diabetes. 2016;65(11):3301-13.
487 9. Musovic S, Komai AM, Said MK, Shrestha MM, Wu Y, Wernstedt Asterholm I, et al.
488 Noradrenaline and ATP regulate adiponectin exocytosis in white adipocytes: Disturbed adrenergic and
489 purinergic signalling in obese and insulin-resistant mice. Mol Cell Endocrinol. 2022;549:111619.
490 10. Mattheyses AL, Simon SM, Rappoport JZ. Imaging with total internal reflection
491 fluorescence microscopy for the cell biologist. J Cell Sci. 2010;123(Pt 21):3621-8.
492 11. Burchfield JG, Lopez JA, Mele K, Vallotton P, Hughes WE. Exocytotic vesicle behaviour
493 assessed by total internal reflection fluorescence microscopy. Traffic. 2010;11(4):429-39.
494 12. Moffat J, Sabatini DM. Building mammalian signalling pathways with RNAi screens.
495 Nature reviews Molecular cell biology. 2006;7(3):177-87.
496 13. Li M, Rossi JJ. Lentiviral vector delivery of siRNA and shRNA encoding genes into
497 cultured and primary hematopoietic cells. Methods in molecular biology. 2008;433:287-99.
498 14. Carlotti F, Bazuine M, Kekarainen T, Seppen J, Pognonec P, Maassen JA, et al. Lentiviral
499 vectors efficiently transduce quiescent mature 3T3-L1 adipocytes. Mol Ther. 2004;9(2):209-17.
500 15. Burgoyne RD, Morgan A. Secretory granule exocytosis. Physiol Rev. 2003;83(2):581-
501 632.
502 16. MacDonald PE, Rorsman P. The ins and outs of secretion from pancreatic beta-cells:
503 control of single-vesicle exo- and endocytosis. Physiology (Bethesda). 2007;22:113-21.
504 17. Garcia AG, Garcia-De-Diego AM, Gandia L, Borges R, Garcia-Sancho J. Calcium signaling
505 and exocytosis in adrenal chromaffin cells. Physiol Rev. 2006;86(4):1093-131.
506 18. Wang ZV, Scherer PE. Adiponectin, the past two decades. J Mol Cell Biol. 2016;8(2):93-
507 100.
508 19. Cong L, Chen K, Li J, Gao P, Li Q, Mi S, et al. Regulation of adiponectin and leptin
509 secretion and expression by insulin through a PI3K-PDE3B dependent mechanism in rat primary
510 adipocytes. Biochem J. 2007;403(3):519-25.

20. Bogan JS, Lodish HF. Two compartments for insulin-stimulated exocytosis in 3T3-L1 adipocytes defined by endogenous ACRP30 and GLUT4. J Cell Biol. 1999;146(3):609-20.
21. Xie L, O'Reilly CP, Chapes SK, Mora S. Adiponectin and leptin are secreted through distinct trafficking pathways in adipocytes. Biochim Biophys Acta. 2008;1782(2):99-108.
22. Lovfors W, Simonsson C, Komai AM, Nyman E, Olofsson CS, Cedersund G. A systems biology analysis of adrenergically stimulated adiponectin exocytosis in white adipocytes. J Biol Chem. 2021;297(5):101221.
23. Zhang X, Heckmann BL, Liu J. Studying lipolysis in adipocytes by combining siRNA knockdown and adenovirus-mediated overexpression approaches. Methods Cell Biol. 2013;116:83-105.
24. Nugent C, Prins JB, Whitehead JP, Savage D, Wentworth JM, Chatterjee VK, et al. Potentiation of glucose uptake in 3T3-L1 adipocytes by PPAR gamma agonists is maintained in cells expressing a PPAR gamma dominant-negative mutant: evidence for selectivity in the downstream responses to PPAR gamma activation. Mol Endocrinol. 2001;15(10):1729-38.
25. Gandasi NR, Vesto K, Helou M, Yin P, Saras J, Barg S. Survey of Red Fluorescence Proteins as Markers for Secretory Granule Exocytosis. PLoS One. 2015;10(6):e0127801.
26. Olofsson CS, Gopel SO, Barg S, Galvanovskis J, Ma X, Salehi A, et al. Fast insulin secretion reflects exocytosis of docked granules in mouse pancreatic B-cells. Pflugers Arch. 2002;444(1-2):43-51.
27. Komai AM, Shrestha MM, Musovic S, Olofsson CS. An Approach to Monitor Exocytosis in White Adipocytes. Methods in molecular biology. 2021;2233:203-22.
28. Park HK, Ahima RS. Resistin in rodents and humans. Diabetes Metab J. 2013;37(6):404-14.
29. Musovic S, Shrestha MM, Komai AM, Olofsson CS. Resistin is co-secreted with adiponectin in white mouse adipocytes. Biochem Biophys Res Commun. 2021;534:707-13.
30. Rogne M, Tasken K. Compartmentalization of cAMP signaling in adipogenesis, lipogenesis, and lipolysis. Hormone and metabolic research = Hormon- und Stoffwechselforschung = Hormones et metabolisme. 2014;46(12):833-40.
31. Calaghan S, Kozera L, White E. Compartmentalisation of cAMP-dependent signalling by caveolae in the adult cardiac myocyte. J Mol Cell Cardiol. 2008;45(1):88-92.
32. Brannmark C, Kay EI, Ortegren Kugelberg U, Chanclon B, Shrestha MM, Wernstedt Asterholm I, et al. Adiponectin is secreted via caveolin 1-dependent mechanisms in white adipocytes. J Endocrinol. 2020;247(1):25-38.
33. Musovic S, Olofsson CS. Adrenergic stimulation of adiponectin secretion in visceral mouse adipocytes is blunted in high-fat diet induced obesity. Sci Rep. 2019;9(1):10680.

Author contributions

MMS and CSO outlined the study and designed the experiments. MMS carried out all experimental work and analysis. CSO and MMS wrote the manuscript. SB provided method and analysis expertise and gave valuable input on the manuscript. All authors approved the final version of the manuscript.

Funding

This study was funded by the Swedish Research Council (2013-07107 and 2019-01239).

556 **Legends**

557 **Fig. 1 Effects of an elevation of cAMP and Ca^{2+} on adiponectin exocytosis in white**
558 **adipocytes.**
559 Forskolin and 3-isobutyl-1-methylxanthine (IBMX) elevate the intracellular concentration of
560 cAMP through the activation of adenylyl cyclase (AC) and inhibition of phosphodiesterase,
561 respectively. The elevation of cAMP results in activation of the downstream target Epac1 and
562 fusion of adiponectin containing vesicles with the plasma membrane with subsequent
563 adiponectin release. Ionomycin, a calcium ionophore, facilitates the transport of Ca^{2+} across
564 the plasma membrane and the elevation in intracellular Ca^{2+} augments the fusion of
565 adiponectin-containing vesicles with the plasma membrane. Ca^{2+} also induces replenishment
566 of release-competent adiponectin vesicles, to maintain secretion of adiponectin over longer
567 time periods.

568

569 **Fig. 2 Expression of adiponectin and shRNA-mediated adiponectin knockdown in 3T3-**
570 **L1 adipocytes.**
571 **A)** Gene expression of endogenous adiponectin in 3T3-L1 cells/adipocytes measured at every
572 48 hours after initiation of differentiation until day 10. Western blot **(B)** and densitometric
573 analysis (**C**) of adiponectin protein expression after shRNA-mediated knockdown of
574 endogenous adiponectin in 3T3-L1 cells. The cells were infected with lenti-virus-expressing
575 control shRNA targeting GFP (scrambled) and two variants of shRNA targeting murine
576 adiponectin (shAcrp30-A and shAcrp30-C), and differentiated into mature adipocytes after
577 puromycin selection. **D)** mRNA levels of adiponectin in shRNA-mediated knockdown
578 compared with control cells. Statistical analysis: Brown-Forsythe and Welch ANOVA tests
579 (Dunnett's T3 multiple comparisons test), assuming unequal SDs at α – level of 0.05 for A and
580 Ordinary One-way ANOVA tests (Dunnett's multiple comparisons test), assuming equal SDs
581 at α – level of 0.05 for C & D. Data are presented as mean ± SEM of three independent
582 experiments. *P<0.05, ***P<0.001 and ****P<0.0001.
583

584 **Fig. 3 Rescue of shRNA-mediated adiponectin knockdown with mCherry fused with**
585 **human adiponectin and estimation of vesicle size**
586 Western blot for **A)** reduced and **B)** non-reduced adiponectin. The expression of mCherry-
587 fused adiponectin in the 3T3-L1 adipocytes was observed under **C)** Fluorescence (Scale
588 bar=100 μm) and **D)** TIRF microscope (Scale bar=10 μm). The 3T3-L1 cells, with shRNA-
589 mediated silencing of endogenous adiponectin expression, were infected with lenti-virus for
590 stably expressing human adiponectin fused with mCherry at C-terminal alone or with FLAG-
591 tag at either C- or N- terminal. The lenti-virus infected cells were differentiated and the over-
592 expression of recombinant adiponectin was analysed. **E-F)** Estimation of adiponectin-mCherry
593 vesicle size (n=267), as described in Methods. Fluorescent polystyrene beads with a diameters
594 of 2, 1, 0.5, 0.2 and 0.1 μm were imaged. Scale bars=10 μm.
595

596 **Fig. 4 TIRF imaging of cAMP-stimulated 3T3-L1 adipocyte adiponectin exocytosis.**
597 3T3-L1 adipocytes stably expressing recombinant adiponectin were serum starved for 30 min
598 at 32^0C and treated with **A**) 10 μM Forskolin and 200 μM IBMX or **B)** DMSO (Control) for
599 15 minutes during which images were taken at 2 FPS using TIRF microscopy. A laser
600 wavelength of 561 nm with exposure time between 30 - 100 ms was used to excite mCherry.

601 Note in inset region at lower panel that some vesicles are released (dotted circles) while others
602 remain stable (whole circles). Scale bar = 10 µm. **C)** Examples of FSK/IBMX-induced single
603 vesicle dynamics over time, in the stimulated adipocyte in (A) and in the control adipocyte in
604 (B). Scale bar = 2 µm. **D-E)** Relative average fluorescence intensity change vs. time in a single
605 vesicle stimulated with FSK/IBMX. **F)** Cumulative frequency of percentage of vesicles
606 released at the end of a 10 min FSK/IBMX stimulation. **G)** Vesicle count before and 15 min
607 after stimulation with FSK/IBMX. Statistical analysis: 2way ANOVA (Sidak's multiple
608 comparisons test). Data are presented as mean ± SEM of eight independent experiments.
609 *P<0.05; **P<0.01.
610
611 **Fig. 5 TIRF imaging of Ca^{2+}-stimulated 3T3-L1 adipocyte adiponectin exocytosis.**
612 3T3-L1 adipocytes stably expressing recombinant adiponectin were serum starved for 30 min
613 at 32^0C and treated with **A)** 1 µM ionomycin or **B)** DMSO (Control) for 15 minutes during
614 which images were taken at 2 FPS using TIRF microscopy. A laser wavelength of 561 nm with
615 exposure time between 30 - 100 ms was used to excite mCherry. Note in inset region at lower
616 panel that some vesicles are released (dotted circles) while others remain stable (whole circles).
617 Scale bar = 10 µm. **C)** Examples of ionomycin-induced single vesicle dynamics over time, in
618 the stimulated adipocyte in (A) and in the control cell in (B). Scale bar = 2 µm. **D-E)** Relative
619 average fluorescence intensity change vs. time in a single vesicle upon ionomycin stimulation.
620 **F)** Cumulative frequency of percentage of vesicles released by ionomycin at the end of 10 min
621 of stimulation. **G)** Vesicles count before and 15 min after stimulation with ionomycin.
622 Statistical analysis: 2way ANOVA (Sidak's multiple comparisons test). Data are presented as
623 mean ± SEM of eight independent experiments. *P<0.05; **P<0.01.
624
625 **Fig.6 cAMP- and Ca^{2+}-stimulated adiponectin secretion in native and adiponectin-**
626 **mCherry-expressing 3T3-L1 adipocytes.**
627 **A)** Native mature 3T3-L1 adipocytes were serum starved for 30 min at 32^0C and treated with
628 DMSO, FSK/IBMX, or ionomycin for 30 min at 32^0C. The extracellular solutions were
629 collected and analysed for endogenous total adiponectin release using ELISA. Statistical
630 analysis: Brown-Forsythe and Welch ANOVA (Dunnett's T3 multiple comparisons test),
631 assuming unequal SDs at α – level of 0.05. N=6 for Control and ionomycin; N= 5 for
632 FSK/IBMX. **B)** Human total adiponectin and **C)** human HMW adiponectin secretion in stably
633 expressing adipocytes, measurement using ELISA. Statistical analysis: Ordinary One-way
634 ANOVA (Holm-Sidak's multiple comparisons test), assuming equal SDs at α – level of 0.05.
635 N= 4. Data are presented as mean ± SEM. *P<0.05, **P<0.01 and ***P<0.001. Lipolysis
636 measured as FFA **D)** and glycerol **E)** release in 3T3-L1 adipocytes stably expressing
637 recombinant adiponectin under DMSO (Control), FSK/IBMX or ionomycin stimulation. Note
638 that only co-stimulation with FSK/IBMX significantly increased the secretion of FFA and
639 glycerol compared to the control. Statistical analysis: Ordinary One-way ANOVA (Dunnett's
640 multiple comparisons test), assuming equal SDs at α – level of 0.05. N=5. Data are presented
641 as mean ± SEM. ****P<0.0001 and ns = non-significant.

642

643

644

645 **Table 1**

Primer	Forward	Reverse
shAcrp30-A	CCGGCTACAACCAACAGAATCATTACTCGAGTAATGATTCTGTTGGTTGTAGTTTTTG	AATTCAAAAACTACAACCAACAGAATCATTACTCGAGTAATGATTCTGTTGGTTGTAG
shAcrp30-B	CCGGGACAAGGCCGTTCTCTTCACCCTCGAGGGTGAAGAGAACGGCCTTGTCTTTTTG	AATTCAAAAAGACAAGGCCGTTCTCTTCACCCTCGAGGGTGAAGAGAACGGCCTTGTC
shAcrp30-C	CCGGCCACAATGGCACACCAGGCCGCTCGAGCGGCCTGGTGTGCCATTGTGGTTTTTG	AATTCAAAAACCACAATGGCACACCAGGCCGCTCGAGCGGCCTGGTGTGCCATTGTGG
Acrp30	CCCAAGGGAACTTGTGCAGGTTGGATG	GTTGGTATCATGGTAGAGAAGAAAGCC
β-Actin	TTCTTTGCAGCTCCTTCG	TTCTGACCCATTCCCACC

646

647 **Supplementary Videos**

648 **Supplementary video 1**

649 3T3-L1 adipocytes stably expressing adiponectin-mCherry were treated with 10 μM Forskolin
650 and 200 μM IBMX for 15 minutes during which images were taken at 2 FPS using TIRF
651 microscopy. The video is condensed to show every 10th frame. Time point of FSK/IBMX
652 addition = 30 s. Scale bar = 10 μm.

653 **Supplementary video 2**

654 3T3-L1 adipocytes stably expressing recombinant adiponectin were treated with DMSO
655 (control for Forskolin/IBMX recording) for 15 minutes during which images were taken at 2
656 FPS using TIRF microscope. The video is condensed to show every 10th frame. Scale bar = 10
657 μm.

658 **Supplementary video 3**

659 3T3-L1 adipocytes stably expressing recombinant adiponectin were treated with 1 μM
660 ionomycin for 15 minutes during which images were taken at 2 FPS using TIRF microscope.
661 The video is condensed to show every 10th frame. Time point of ionomycin addition = 30 s.
662 Scale bar = 10 μm.

663 **Supplementary video 4**

664 3T3-L1 adipocytes stably expressing recombinant adiponectin were treated with DMSO
665 (control for ionomycin recording) for 15 minutes during which images were taken at 2 FPS
666 using TIRF microscope. The video is condensed to show every 10th frame. Scale bar = 10 μm.

667

668 **Abbreviation**

669 AAV = Adeno-Associated Virus

670 ANOVA = Analysis of variance

671 ATCC = American Type Culture Collection

672 cAMP = Cyclic Adenosine Monophosphate
673 CMV = Cytomegalovirus
674 DMEM = Dulbecco's Modified Eagle Medium
675 DMSO = Dimethyl sulfoxide
676 EDTA = Ethylenediaminetetraacetic acid
677 EGFP = Enhanced Green Fluorescent Protein
678 ELISA = Enzyme-linked immunosorbent assay
679 Epac1 = Exchange factor directly activated by cAMP 1
680 Epac2 = Exchange factor directly activated by cAMP 2
681 EC = Extracellular
682 FBS = Fetal bovine serum
683 FPS = Frames per second
684 FSK = Forskolin
685 GFP = Green Fluorescent Protein
686 HMW = High Molecular Weight
687 IBMX = 3-isobutyl-1-methylxanthine
688 NPY = Neuropeptide Y
689 NS = Not significant
690 PAGE = Polyacrylamide gel electrophoresis
691 PVDF = Polyvinylidene fluoride
692 qPCR = quantitative polymerase chain reaction
693 ROI = Region of interest
694 SD = Standard deviation
695 SDS = Sodium dodecyl-sulfate
696 SEM = Standard error of mean
697 shRNA = short hairpin ribonucleic acid
698 TIRF = Total internal reflection fluorescence
699

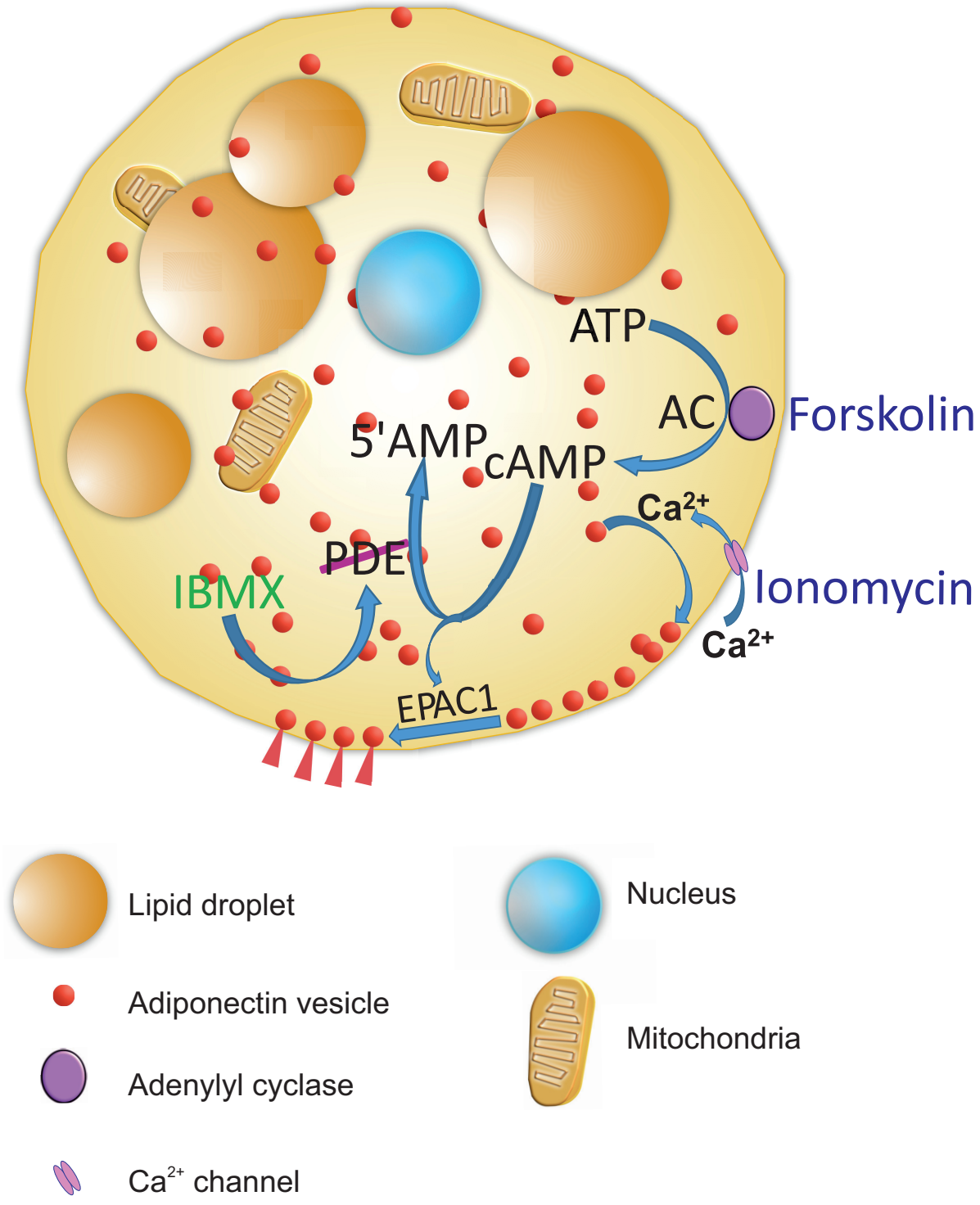
ATP
AC
Forskolin
5'AMP
cAMP
Ca2+
PDE
IBMX
Ionomycin
Ca2+
EPAC1
Lipid droplet
Nucleus
Adiponectin vesicle
Mitochondria
Adenylyl cyclase
Ca2+ channel

Fig. 1

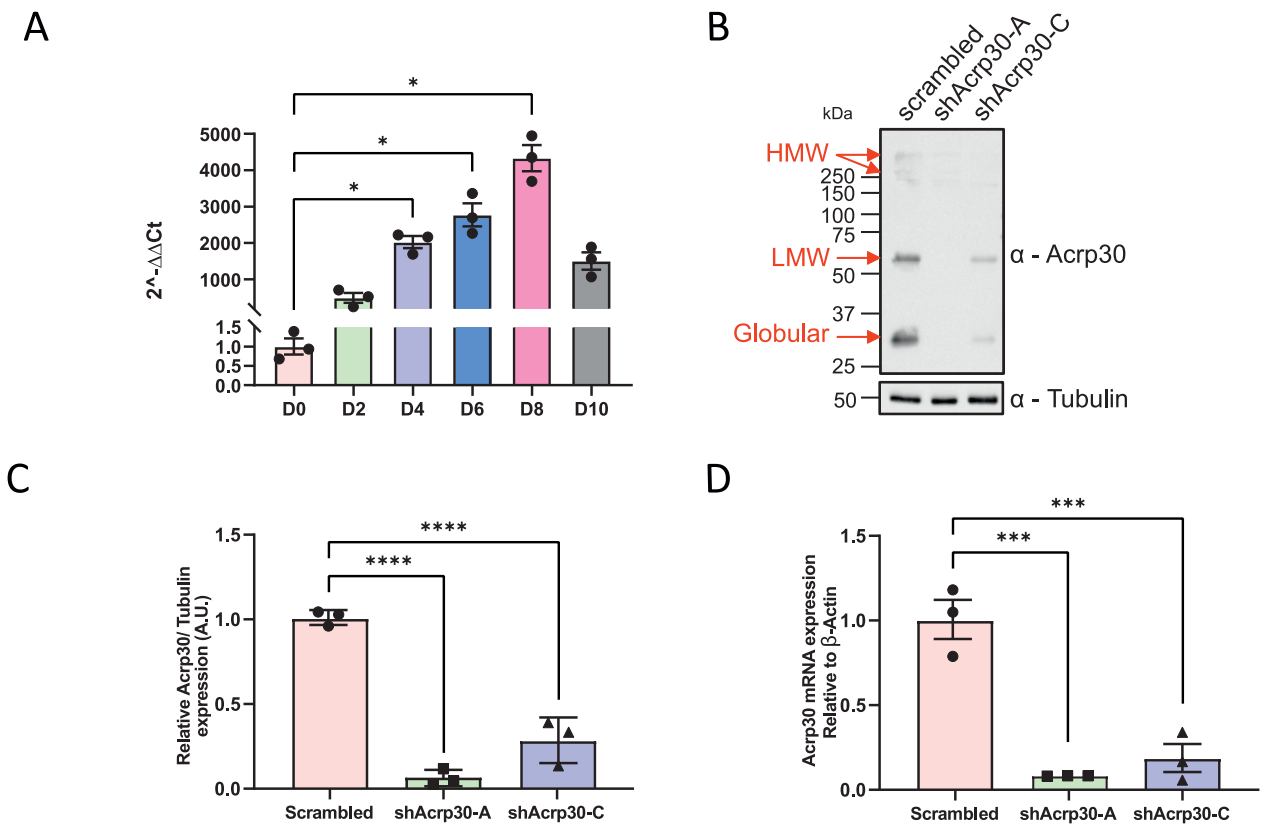
A
2^-ΔΔCt
5000
4000
3000
2000
1000
1.5
1.0
0.5
0.0
D0
D2
D4
D6
D8
D10
B
scrambled
shAcrp30-A
shAcrp30-C
kDa
HMW
250
150
100
75
LMW
50
37
Globular
25
50
α - Acrp30
α - Tubulin
C
Relative Acrp30/ Tubulin expression (A.U.)
Scrambled
shAcrp30-A
shAcrp30-C
D
Acrp30 mRNA expression Relative to β-Actin
Scrambled
shAcrp30-A
shAcrp30-C

Fig. 2

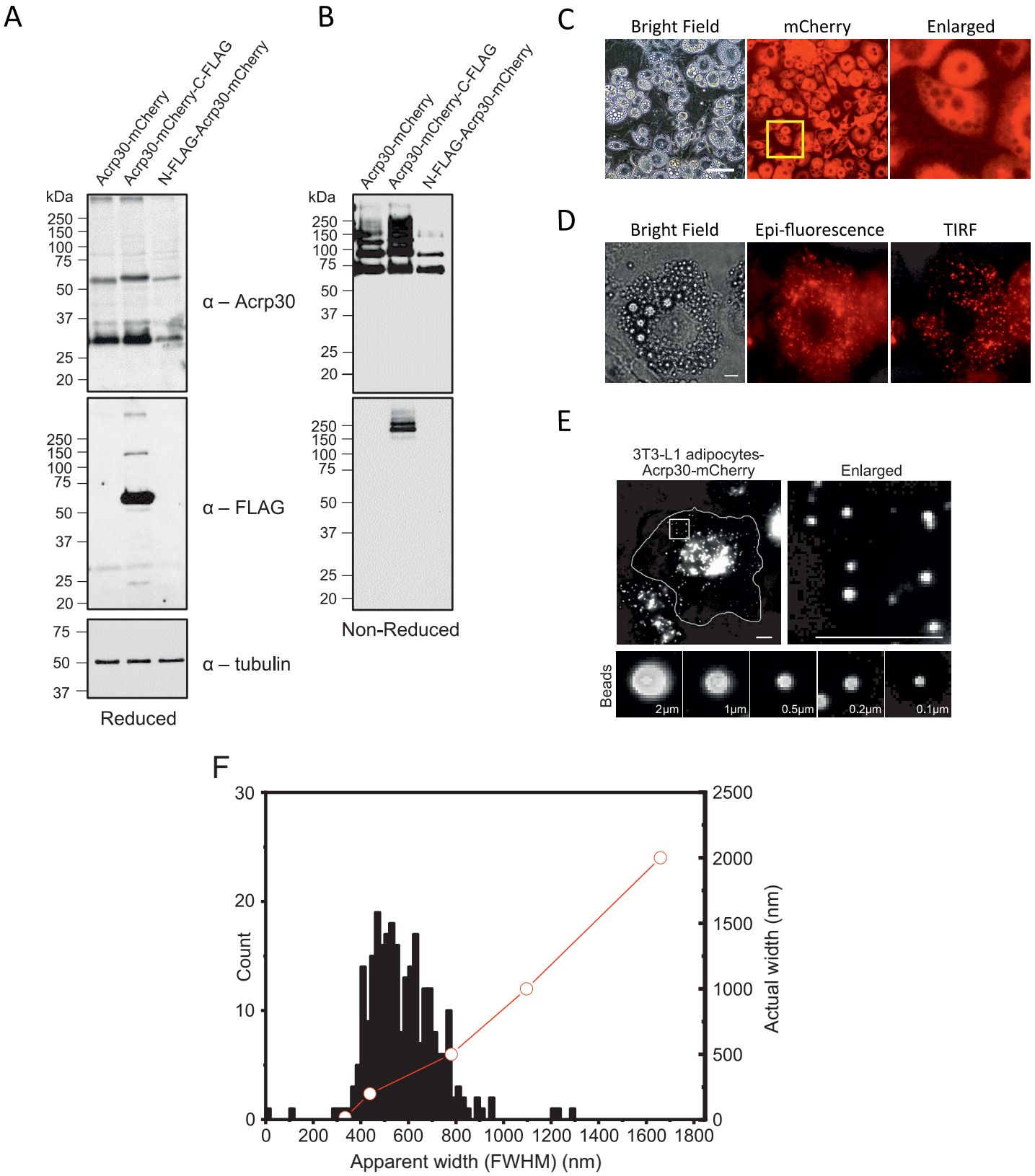
A
Acrp30-mCherry
Acrp30-mCherry-C-FLAG
N-FLAG-Acrp30-mCherry
kDa
250
150
100
75
50
37
25
20
α – Acrp30
α – FLAG
α – tubulin
Reduced
B
Non-Reduced
C
Bright Field
mCherry
Enlarged
D
Bright Field
Epi-fluorescence
TIRF
E
3T3-L1 adipocytes-
Acrp30-mCherry
Enlarged
Beads
2μm
1μm
0.5μm
0.2μm
0.1μm
F
Count
Actual width (nm)
Apparent width (FWHM) (nm)
0
200
400
600
800
1000
1200
1400
1600
1800
500
1500
2000
2500
10
20
30

Fig. 3

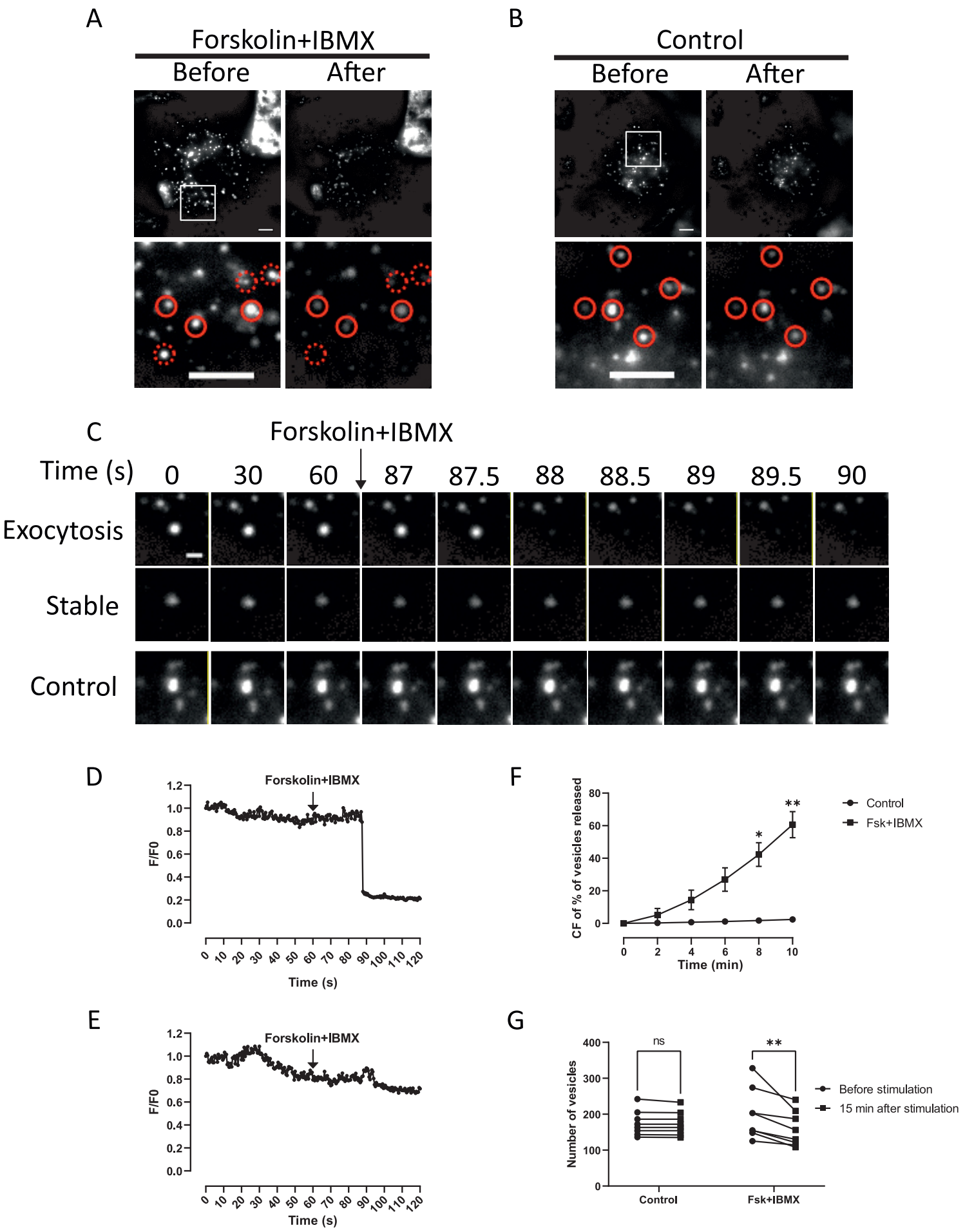
A
Forskolin+IBMX
Before
After
B
Control
Before
After
C
Forskolin+IBMX
Time (s)
0
30
60
87
87.5
88
88.5
89
89.5
90
Exocytosis
Stable
Control
D
Forskolin+IBMX
F/F0
Time (s)
E
Forskolin+IBMX
F/F0
Time (s)
F
CF of % of vesicles released
Time (min)
Control
Fsk+IBMX
G
Number of vesicles
ns
**
Control
Fsk+IBMX
Before stimulation
15 min after stimulation

Fig. 4

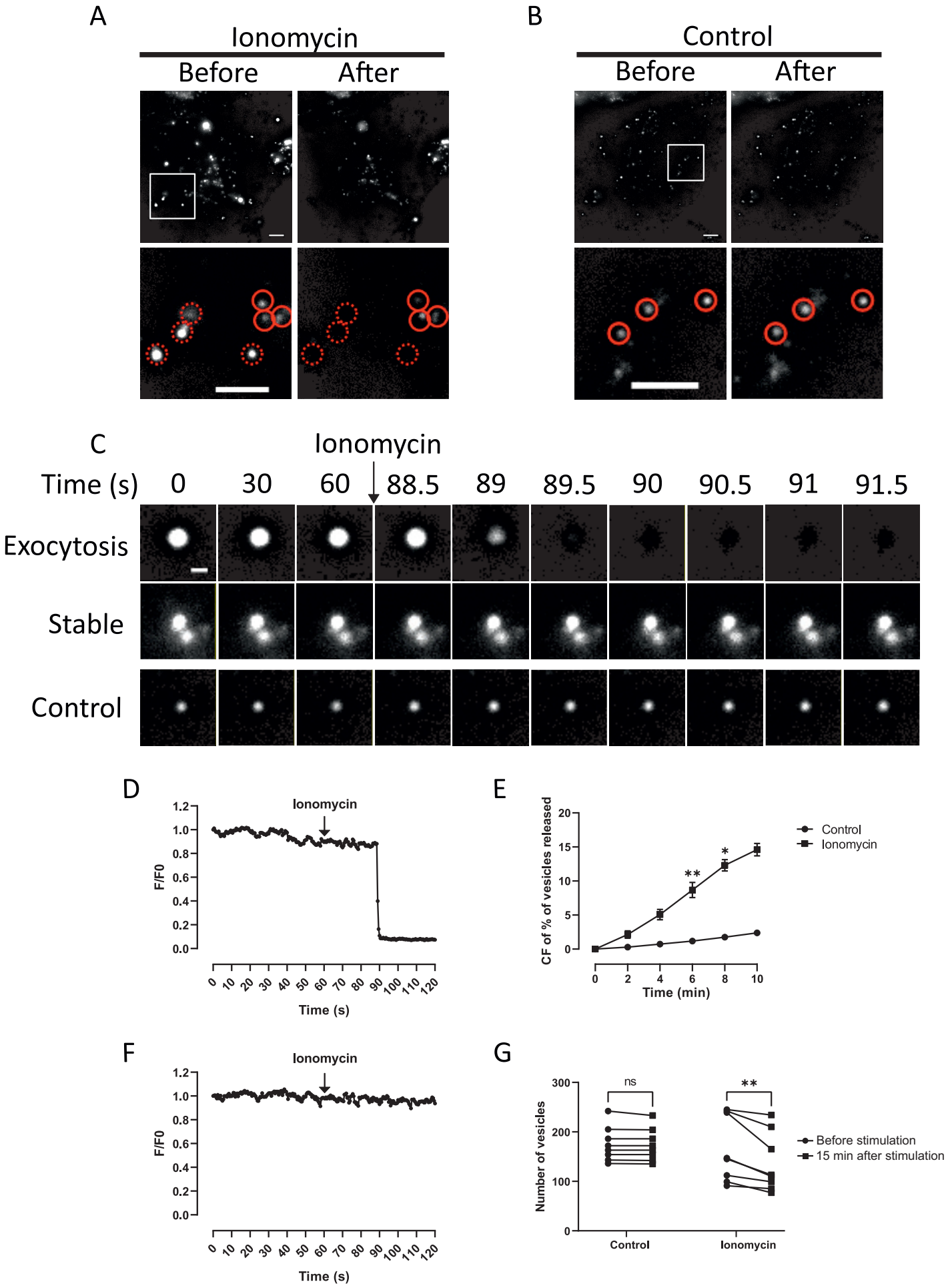
A
Ionomycin
Before
After
B
Control
Before
After
C
Ionomycin
Time (s)
0
30
60
88.5
89
89.5
90
90.5
91
91.5
Exocytosis
Stable
Control
D
Ionomycin
F/F0
Time (s)
E
CF of % of vesicles released
Time (min)
Control
Ionomycin
**
*
F
Ionomycin
F/F0
Time (s)
G
Number of vesicles
ns
**
Control
Ionomycin
Before stimulation
15 min after stimulation

Fig. 5

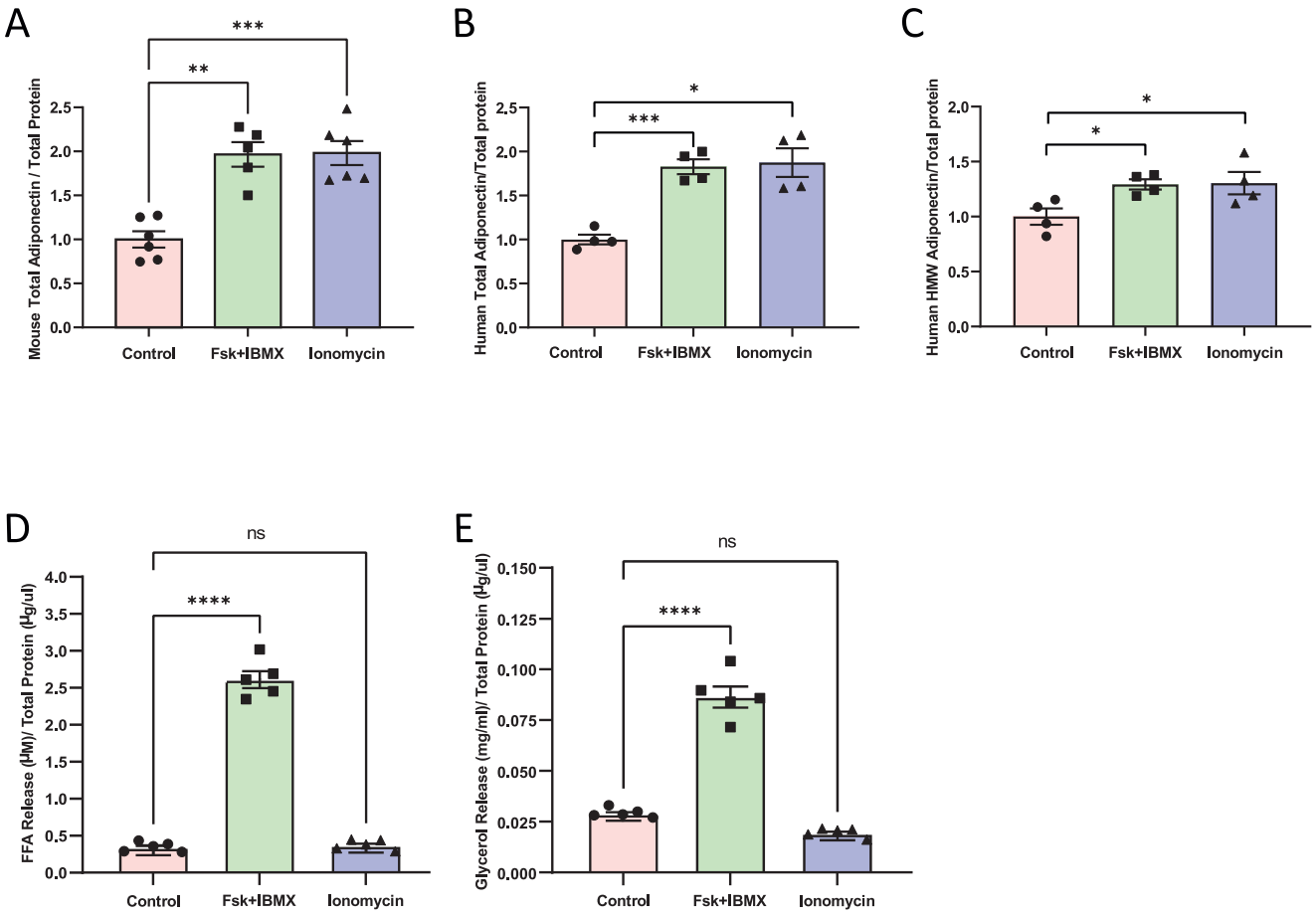
A
Mouse Total Adiponectin / Total Protein
***
**
Control
Fsk+IBMX
Ionomycin
B
Human Total Adiponectin/Total protein
*
***
Control
Fsk+IBMX
Ionomycin
C
Human HMW Adiponectin/Total protein
*
*
Control
Fsk+IBMX
Ionomycin
D
FFA Release (μM)/ Total Protein (μg/ul)
ns
****
Control
Fsk+IBMX
Ionomycin
E
Glycerol Release (mg/ml)/ Total Protein (μg/ul)
ns
****
Control
Fsk+IBMX
Ionomycin

Fig. 6

Supplementary Fig 1

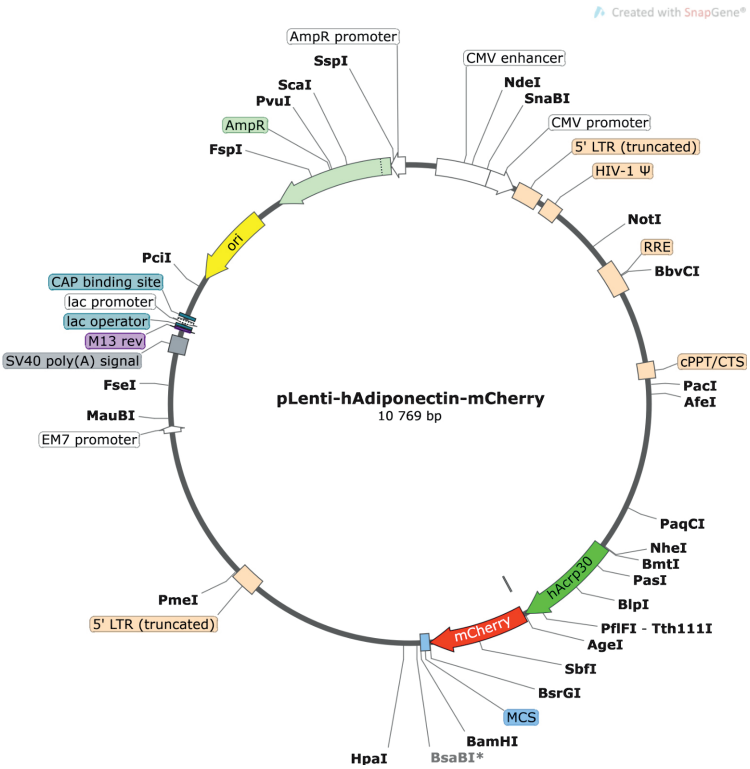

Plasmid map of lenti-viral construct for human adiponectin fused with mCherry at C-terminal created with SnapGene. 3T3-L1 adipocytes expressing recombinant adiponectin were serum starved for 30 minutes at 32 ^{0}C and treated with 10 μM Forskolin and 200 μM IBMX, 1 μM ionomycin and DMSO as Control for 15 minutes at 32 ^{0}C during which images were taken at 2 FPS using TIRF microscope.